Engineering 53 (2025) 203–213

Contents lists available at ScienceDirect

Engineering

journal homepage: www.elsevier.com/locate/eng

Research
Environmental Engineering—Article

Bank Filtration as a Robust Pretreatment of Gravity-Driven Membrane Filtration: Performance Enhancement and Mechanistic Insights

Na Li [a], Chu Zhou [a], Fang Xu [b], Danting Shi [a], Fanxi Zeng [a], Liang Luo [a], Zheng Fang [a], Senlin Shao [a,*]

[a] School of Civil Engineering, Wuhan University, Wuhan 430072, China
[b] Faculty of Resources and Environmental Science, Hubei University, Wuhan 430062, China

ARTICLE INFO

Article history:
Received 26 January 2024
Revised 9 August 2024
Accepted 6 January 2025
Available online 18 January 2025

Keywords:
Gravity-driven membrane
Bank filtration
Biofilm
Membrane fouling
Biological stability

ABSTRACT

A gravity-driven membrane (GDM) system is a cleaning-free ultrafiltration (UF) process for decentralized water purification. However, GDM has a poor permeate quality and low stable flux when the feed water contains high levels of particulates, organic matter, and micropollutants. To address these challenges, this study used riverbank filtration (BF) as a pretreatment for GDM. The experimental results showed that BF could effectively reduce turbidity and particulate organic matter, and preferentially remove biopolymers and protein-like fluorescent components from natural organic matter. The removal efficiencies of micropollutants (diclofenac, carbamazepine, acetamidophenol, and bisphenol A) increased by 15.2%–65.3% in the presence of BF. Moreover, BF-GDM improved the removal of assimilable organic carbon (AOC) by 42%, thereby enhancing the biological stability of the permeate. Despite a modest increase of approximately 20% in the removal of dissolved organic matter, the BF significantly improved the stable flux from 2.8 to 7.3 $L{\cdot}m^{-2}{\cdot}h^{-1}$. This remarkable improvement is attributed to the effective removal of key foulants, including particulate substances, biopolymers, and protein-like fluorescent substances, which leads to a thinner bio-cake layer with a higher density of microorganisms. Additionally, because of the high microbial diversity of the soil, BF pretreatment enriched the microbial diversity of the bio-cake layer, thereby enriching functional microorganisms capable of degrading pollutants in BF-GDM, such as Nitrospirota and Ascomycota. Overall, BF is a highly effective pretreatment for GDM, which potentially broadens its application to polluted source water.

© 2025 THE AUTHORS. Published by Elsevier LTD on behalf of Chinese Academy of Engineering and Higher Education Press Limited Company. This is an open access article under the CC BY license (http://creativecommons.org/licenses/by/4.0/).

1. Introduction

Gravity-driven membrane (GDM) filtration, also known as "biofilm-controlled ultrafiltration (UF)," represents a low-maintenance decentralized membrane process [1]. The key feature of GDM is that it can maintain a consistent permeate flux of several liter per square meter per hour for months to years without physical or chemical cleaning [2]. This cleaning-free feature is primarily attributed to the self-adjustment of the bio-cake layer in GDM. Specifically, the composition of the bio-cake can be balanced by microbial biodegradation, whereas the structure of the bio-cake can be engineered through eukaryotic activity [2]. Consequently, the bio-cake may maintain a stable composition and loose structure, thereby avoiding a continuous increase in cake fouling resistance. GDM is an effective membrane process for decentralized drinking water treatment and has been successfully implemented in several regions, including South Africa and Kenya [3,4].

However, GDM faces challenges when treating polluted source waters. First, GDM may produce poor-quality source water containing elevated concentrations of dissolved pollutants, such as dissolved organic matter and micropollutants. For example, the permeate exhibits higher dissolved organic carbon (DOC) than the feed water [5,6]. The removal rate of micropollutants, including sulfamethoxazole and diclofenac, can also be lower than 10% [7]. Second, GDM may have an ultralow stable flux and is usually less than 3 $L{\cdot}m^{-2}{\cdot}h^{-1}$ when the source water contains high concentrations of particles, organic matter, and algal cells [8]. For example, when fed with high-turbidity source water (> 600 nephelometric turbidity units (NTU)), the stable flux of GDM experienced an irreversible drop from 4–6 to 2–4 $L{\cdot}m^{-2}{\cdot}h^{-1}$ [4]. With an increase in DOC concentration from 2 to 7 $mg{\cdot}L^{-1}$, the stable flux decreased from 7 to 2 $L{\cdot}m^{-2}{\cdot}h^{-1}$ [4,6,9–12]. Suitable pretreatments can be

* Corresponding author.
E-mail address: shaosenlin@whu.edu.cn (S. Shao).

https://doi.org/10.1016/j.eng.2025.01.003
2095-8099/© 2025 THE AUTHORS. Published by Elsevier LTD on behalf of Chinese Academy of Engineering and Higher Education Press Limited Company.
This is an open access article under the CC BY license (http://creativecommons.org/licenses/by/4.0/).

added to enhance the capability of GDM to treat polluted source water. These pretreatments should align with the principles of decentralized water treatment, including being chemical-free and low-maintenance, because GDM generally serves as a decentralized water treatment process. Consequently, conventional pretreatments involving the addition of chemicals and complex operations such as coagulation and oxidation [13,14] may not be suitable for GDM systems.

Bank filtration or riverbank filtration (BF) is a simple and low-maintenance process that involves the construction of extraction wells along the natural banks of rivers or lakes. As water flows through the soil of banks, suspended particles, algae, and organic compounds are removed through mechanisms such as soil adsorption and microbial degradation. The operational principles of biofiltration are similar to the BF mechanism and are increasingly used for pretreating drinking water [15,16]. Biofiltration can effectively remove various organic pollutants from water [17,18]. However, biofiltration as a pretreatment poses the risk of clogging, necessitating regular maintenance or media replacement, which results in higher operational costs [19,20]. BF is a low-maintenance, green water treatment technology that does not require chemical additions [21,22]. Hallé et al. [23] indicated that BF could effectively achieve low effluent turbidity (< 5 NTU) when dealing with high-turbidity river water (> 1500 NTU). Moreover, DOC was significantly reduced by the biodegradation and adsorption of BF systems [24–26]. The high removal efficiency of biopolymers (40%–60%) has also been reported [27–29]. Therefore, we propose BF as a pretreatment method for GDM to treat polluted source water with high turbidity, organic compounds, and other pollutants. However, the use of BF as a pretreatment for GDM has rarely been reported, and further research is needed to clarify its role in improving GDM performance and to understand its underlying mechanisms.

In this study, we investigated the feasibility of BF as a pretreatment for GDM to improve permeate quality and increase stable flux. The pollutant removal efficiency, biological stability of the permeate, and stable flux in BF-GDM were systematically investigated and benchmarked against those of conventional GDM. The mechanisms of improved performance are discussed by examining the removal of key foulants and the transformation of the microbial community. The results demonstrated that BF pretreatment significantly improved water quality and tripled the stable flux. This study offers a fresh perspective to the utilization of GDM in polluted source waters.

2. Materials and methods

2.1. Materials

2.1.1. Feedwater

The feedwater was sourced from East Lake (Wuhan, China), which is a polluted water source. Water turbidity typically ranges from 3 to 4 NTU, but can exceed 20 NTU during rainy days. The influent had DOC ranging from 7.5 to 8.3 $mg·L^{-1}$, ultraviolet absorbance at 254 nm (UV_{254}) from 0.060 to 0.082 cm^{-1}, total nitrogen (TN) at 1.17 $mg·L^{-1}$, and ammonia nitrogen (NH_4^+-N) at 0.55 $mg·L^{-1}$. These organic indicators were approximately three-fold higher than those found in typical drinking water [30]. To verify the removal of micropollutants, diclofenac, carbamazepine, acetamidophenol, and bisphenol A were introduced into the feedwater at concentrations of 41.8, 17.7, 35.4, and 67.6 $μg·L^{-1}$, respectively, during days 142 to 151. Next, 0.03 $g·L^{-1}$ of methanol solution was introduced into the influent on days 142–151. The water temperature was regulated to remain within 19–25 °C.

2.1.2. Membrane and membrane module

A polyethersulfone flat-sheet UF membrane (Microdyn–Nadir, Germany) with a permeance of 790 $L·m^{-2}·h^{-1}·bar^{-1}$ was used in the filtration process. The membranes were cleaned for 12 h before use by soaking them in a 25% isopropanol solution and then rinsing them in filtered water for another 12 h [3]. Each membrane has a filtration area of 33.2 cm^2.

2.2. Experimental setups

The experimental configuration is depicted in Fig. 1. A black acrylic column was used to simulate BF conditions. The BF column was a cylinder with dimensions of 100 cm × 5.9 cm (height × inner diameter) [31]. The effective volume of the BF column was 2.7 L. Soil was gathered from a depth of 10 cm along the bank of East Lake. Large organic particles such as tree roots were removed. The columns were filled and compacted with soil, and the residual air in the columns was eliminated [32]. To form the BF-GDM system, a peristaltic pump (BT100-2J, Longer Pump Company, China) with a flow rate of 2.5 $mL·min^{-1}$ was employed to transfer feed water from the bottom to the top of the BF column, where it then entered the GDM module. Simultaneously, another portion of the feed water was fed directly into the GDM module, forming the control-GDM. The control-GDM and BF-GDM systems were set to a water head of 60 cm. The empty-bed contact time was adjusted to 18.75 h using a peristaltic pump. The GDM system operated with a hydraulic retention time of 1.25 h.

2.3. Organic matter analysis

To investigate the variation in fluorescent substances in the GDM systems, fluorescence excitation–emission matrices (EEMs) of water samples from both the BF-GDM and control-GDM systems were acquired using a fluorescence spectrophotometer (F-7000, Hitachi Ltd., Japan) and analyzed with parallel factor analysis (PARAFAC) [33] using MATLAB R2019a (MathWorks, USA).

To further reveal the characteristics of the organic substances, their molecular weight distributions were analyzed using a high-performance liquid chromatography system (Waters E2695, Waters, USA). The filtrate sample was separated by size exclusion chromatography using different organic compounds [27,34].

2.4. Biological stability assessment

Assimilable organic carbon (AOC) is widely used to assess water biostability and accounts for a minor part of the DOC in feed water, typically from 0.1% to 9% [35,36]. AOC was measured using a flow cytometer (Accuri C6, BD, USA). The water samples were incubated under controlled conditions with an indigenous bacterial inoculum (i.e., bacteria from East Lake) [36,37]. Specifically, after filtration through 0.22 μm membranes and pasteurization, 20 mL of filtered water was combined with 1 mL of the natural community from East Lake in a carbon-free bottle, then incubated at 30 °C for 72 h [38]. Sodium acetate was used as the standard for AOC, and the standard curve is shown in Fig. S1 in Appendix A.

Phosphorus (P) is a vital element required by all cells and affects microbial growth in aquatic systems [39]. Sufficient P promotes biomass growth [40], thereby increasing the risk of bacterial regrowth in drinking water. Total phosphorus (TP) was used to quantify the level of P and was measured using standard methods [41].

2.5. Fouling resistance calculation

Fouling resistance was assessed using the following formulas:

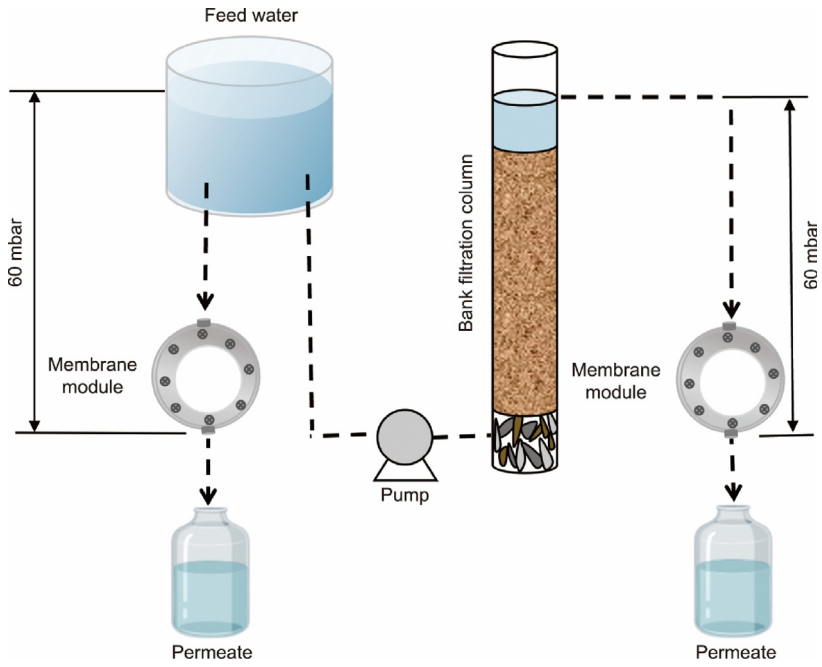

Fig. 1. Diagram of the laboratory-scale setups for the control-GDM (left) and BF-GDM (right) systems.

$$J = \frac{\mathrm{TMP}}{\mu R_t} \quad (1)$$

$$R_t = R_m + R_c + R_p \quad (2)$$

The permeate flux J ($m \cdot s^{-1}$) was calculated based on the daily volume of water produced. The transmembrane pressure (TMP) was maintained at 6 kPa, and μ represents the dynamic viscosity of water (Pa·s). R_m and R_t (m^{-1}) are the hydraulic resistances of the membrane in its virgin and fouled state, respectively. R_c (m^{-1}) represents the resistance due to the bio-cake layer, and R_p (m^{-1}) indicates the resistance from pore blockage and constriction. To determine these resistances, R_m, R_t, and R_m + R_p were measured by filtering Milli-Q water through new membranes, fouled membranes, and membranes that had removed bio-cake layer, respectively. Subsequently, R_p and R_c were derived using Eq. (2).

2.6. Bio-cake layer characterization

In general, denser cake layers typically exhibit higher hydraulic resistance. To analyze the bio-cake layer's morphology, optical coherence tomography (OCT; GAN210C1, Thorlabs, USA) was employed, with ten uniformly spaced spots on the membrane surface being assessed for each observation.

After 188 days of filtration, the total microbial content in the cake layer was measured using adenosine triphosphate (ATP) [42]. A luminometer (GloMax 20/20, Promega, USA) and an ATP detection kit (BioThema Biotechnology, China) were used to measure ATP concentrations [9]. Furthermore, the amounts of polysaccharides and proteins were combined to determine the extracellular polymeric substances (EPS). The determination of polysaccharides and proteins followed the methods outlined in this study [43].

2.7. Microbial community analysis

After filtration, the biofilms collected on the membranes were subjected to microbial analysis. DNA extraction was extracted with the Power Soil DNA Kit (OMEGA, Georgia, USA). Primers 338F and 806R were used to amplify the V3 and V4 sections of the 16S ribosomal ribonucleic acid (rRNA) gene, while primers 528F and 706R were used to amplify the V4 region of the 18S rRNA gene for eukaryotes in the bio-cake layers. Sequencing was carried out on the Illumina HiSeq platform. Clustering analysis of the microbial communities was conducted and visualized using the "ggtree" package, and canonical correspondence analysis (CCA) was performed with R version 4.0.5.

2.8. Other analysis

In all samples, the DOC was separated from particulate organic carbon (POC) by filtration through 0.45 μm filter membranes. The subsamples were kept unfiltered for the total organic carbon (TOC) analysis. DOC and TOC were measured using a TOC analyzer (Multi N/C 2100, Jena, Germany). POC concentrations were calculated as the difference between TOC and DOC. Ultraviolet absorbance (UV_{254}) was measured with a UV/visible spectrophotometer (PGENERAL, China), while turbidity was analyzed using a turbidity meter (2100N, Hach, USA). A high-performance liquid chromatography system (HPLC 1220 Infinity II, Agilent, USA) was used to assess the concentrations of micropollutants. The removal efficiency (R, the subscripts represent the corresponding process) of micropollutants from the permeate was calculated using the formula provided:

$$R_{BF}\,(\%) = \left(\frac{C_0 - C_b}{C_0}\right) \times 100\% \quad (3)$$

$$R_{GDM}\,(\%) = \left(\frac{C_0 - C_m}{C_0}\right) \times 100\% \quad (4)$$

$$R_{\text{BF-GDM}}\,(\%) = \left(\frac{C_b - C_n}{C_b}\right) \times 100\% \quad (5)$$

where C_0 is the concentration of the micropollutants in the influent, and C_b, C_m, and C_n are the concentrations of the micropollutants in the permeates of BF, GDM, and BF-GDM, respectively.

3. Results and discussion

3.1. Enhancing permeate quality by BF pretreatment

3.1.1. Turbidity, particulate organic matter, and dissolved organic matter

Fig. 2 shows the removal of turbidity, POC, and dissolved organic compounds (quantified using DOC and UV_{254}) from the control-GDM and BF-GDM systems. Because of the significant particle rejection capability of UF membranes [6], both control-GDM and BF-GDM achieved very low permeate turbidity (< 0.2 NTU), and no significant difference was found in turbidity removal between the two GDM systems. The BF column reduced the turbidity by 55.3% when used as a filtration system. Even when the influent turbidity reached hundreds to thousands of NTU, such as during heavy rainfall, the BF system was still able to maintain low turbidity levels of several NTU [44]. This efficient removal of turbidity can prevent irreversible flux losses in GDM using high-turbidity raw water [4]. Furthermore, the BF column reduced POC by 62.0% (Fig. 2(b)), possibly by depth filtration and biological degradation [45]. Reducing particulate organic matter can alleviate membrane fouling, thereby improving the quality of the permeate water [5,37,45]. Similar to previous studies [46,47], the control-GDM system showed limited effectiveness in removing dissolved organic matter, achieving removal efficiencies of 15.9% and 4.7% for UV_{254} (Figs. 2(c) and (d)). The low removal could be ascribed to the low rejection of UF by dissolved organic matter [47]. However, BF pretreatment significantly enhanced the DOC and UV_{254} removal in the BF-GDM system by more than 30%. The DOC and UV_{254} levels in the GDM permeate showed a slight decrease of less than 5% compared to the feed (BF effluent), suggesting that biofiltration played a predominant role in organic matter removal within the BF-GDM system. In a BF column, organic substances can be adsorbed or biodegraded [45], thereby improving the removal of organic substances.

3.1.2. Different components of dissolved organic matter

As dissolved organic matter significantly influences water quality and membrane fouling, we conducted further analyses to evaluate the removal efficiency of organic components with varying fluorescence properties and molecular weights (Fig. 3). PARAFAC analysis revealed three fluorescent components: C1 exhibits two excitation peaks at 240 and 310 nm, along with a broad emission spectrum centered between 400 and 450 nm, which is linked to humic-like substances derived from microbial sources. C2 shows double excitation maxima at 270 and 360 nm, with a single emission peak at 470 nm, indicative of humic-like matter originating from terrestrial sources; and C3 displays a primary excitation peak around 225 nm and a secondary peak at approximately 280 nm,

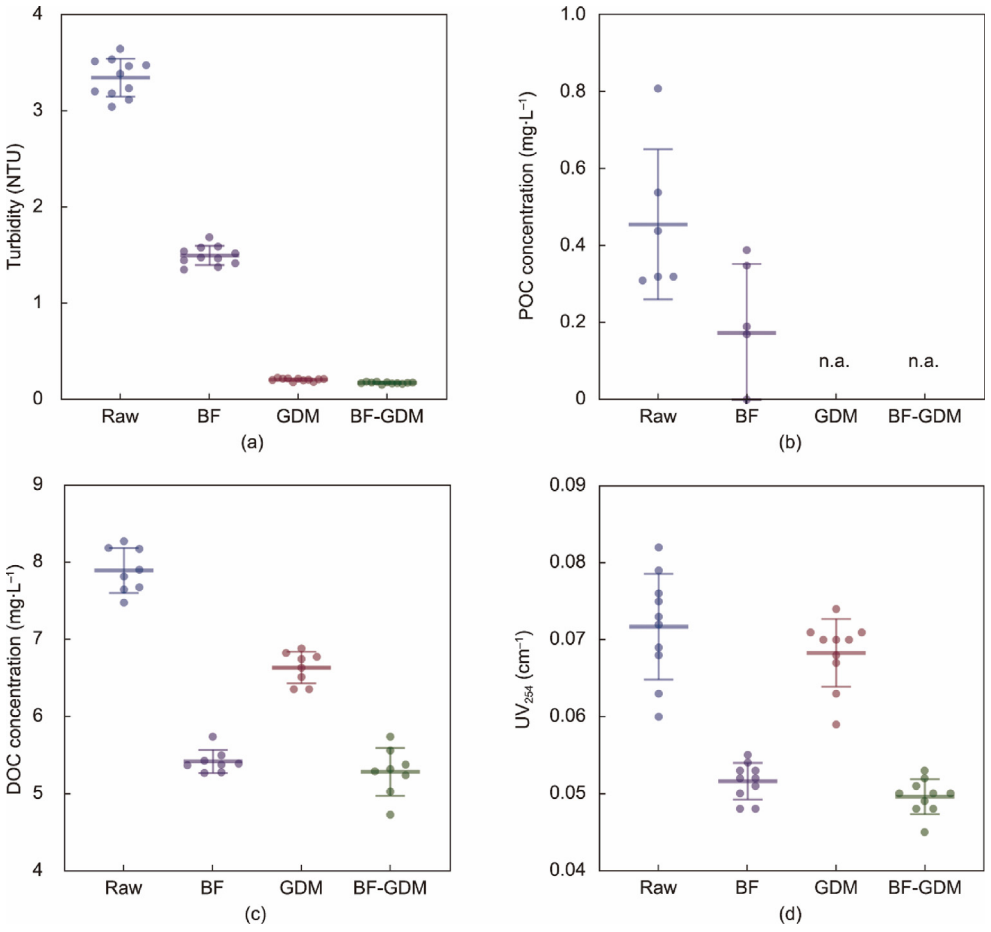

Fig. 2. Water quality of the feedwater, effluent from raw, the BF, and the permeate of the GDM systems. (a) Turbidity, (b) POC, (c) DOC, and (d) UV_{254}. Samples were regularly collected after the flux of the GDM systems was stable. Particulate organic matter was not detected in the permeate of control-GDM and the BF-GDM, and thus, the relevant data were not available (n.a.). Horizontal lines in the *x*-axis direction represent the median of the data set.

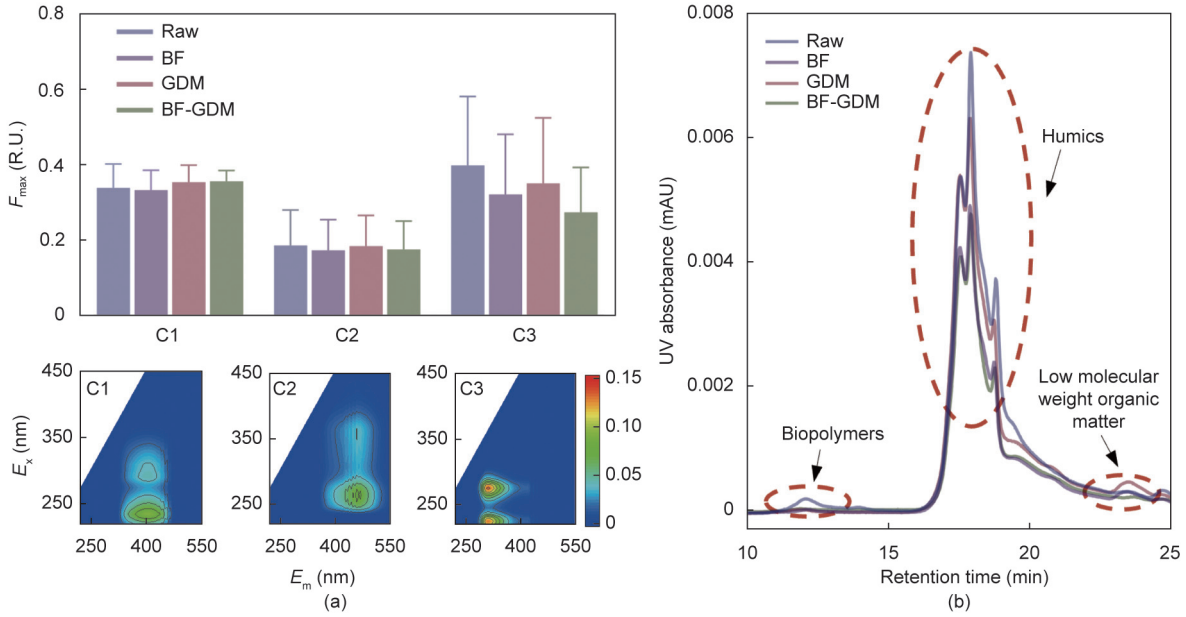

Fig. 3. Components of dissolved organic matter in the control-GDM and BF-GDM. (a) Fluorescent components; (b) organic components with different molecular weights. n = 6, error bars represent the standard deviation. E_x and E_m represent excitation wavelength and emission wavelength, respectively; C1 represents humic-like substances derived from microbial sources; C2 represents humic-like substances originating from terrestrial sources; C3 represents protein-like substances. F_{max} represents the maximum fluorescence intensity, indicating the concentration of the fluorescent components; R.U. represents relative fluorescence intensity (relative units).

corresponding to protein-like substances (Fig. 3(a)) [33]. In both the control-GDM and BF-GDM systems, fluorescence intensities for C1 and C2 showed minimal changes, indicating that the BF column and GDM filtration were not effective in removing humic substances [48]. The low removal efficiency of humic-like substances can be attributed to their small molecular size and low degradability [49]. Unlike the poor removal efficiencies of C1 and C2, the removal efficiencies for C3 in the control-GDM and BF-GDM systems were 12.0% and 31.2%, respectively. According to previous studies [14,50], protein-like C3 can accumulate on membranes, resulting in severe organic fouling. Therefore, the high removal of protein-like C3 with BF pretreatment may reduce organic fouling in the subsequent GDM.

The molecular weight distributions of the dissolved organic substances in both control-GDM and BF-GDM are shown in Fig. 3(b). Peaks related to macromolecular biopolymers were detected in the raw water [29], whereas both BF and GDM filtration markedly reduced the peak intensity of the biopolymers. Biopolymers are characterized by their high molecular weight and biodegradability [28], which make them either efficiently rejected through UF membranes or easily removed by BF. Considering that the rejected biopolymers could be the major foulants of UF membranes [27,29], the pre-removal of biopolymers by BF could substantially reduce membrane fouling. For humic substances, BF-GDM showed a slightly higher removal rate than control-GDM, but the overall removal efficiencies were not high. Notably, the control-GDM permeate had higher levels of low-molecular-weight organic compounds, as indicated by a greater peak intensity at a retention time of 24 min. This may be attributed to the biodegradation of high-molecular-weight organic substances into low-molecular-weight ones within the bio-cake layer of GDM [27].

3.1.3. Micropollutants

The control-GDM exhibited minimal removal efficiencies (< 5%) for diclofenac, carbamazepine, acetamidophenol, and bisphenol A (Fig. 4), suggesting that either the UF membrane did not efficiently remove these pollutants or the microorganisms in the bio-cake did not biodegrade them. With BF pretreatment, the micropollutant removal efficiencies significantly improved. BF-GDM increased the removal of diclofenac, carbamazepine, acetamidophenol, and bisphenol A by 15.2%, 27.5%, 65.3%, and 26.5%, respectively, compared with the control. However, the removal efficiencies of bisphenol A, carbamazepine, and diclofenac were below 30%. These substances are difficult to biodegrade and are typically removed by adsorption [51,52]. However, the removal efficiency of acetamidophenol was the highest in BF-GDM (> 65%). The higher removal of acetamidophenol is attributed to its ability to be degraded by microorganisms [53,54]. The BF column significantly contributed to the removal of micropollutants, and it could remove these substances through adsorption and biodegradation [21,22]. Therefore, BF pretreatment can enhance the water quality of GDM when the raw water contains excessive levels of micropollutants.

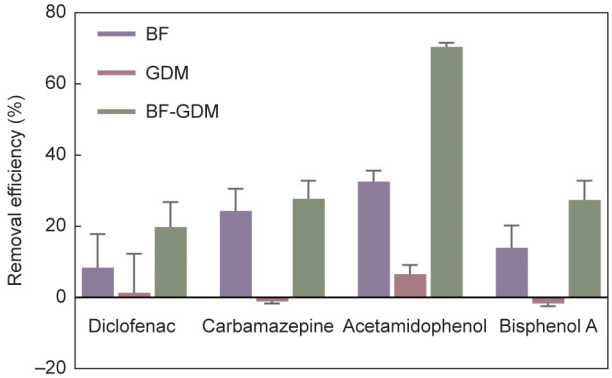

Fig. 4. Efficiency of micropollutant removal in the control-GDM and BF-GDM. Concentration of diclofenac, carbamazepine, acetamidophenol, and bisphenol A in the feed water was 41.8, 17.7, 35.4, and 67.6 $\mu g \cdot L^{-1}$, respectively. n = 3, error bars represent the standard deviation.

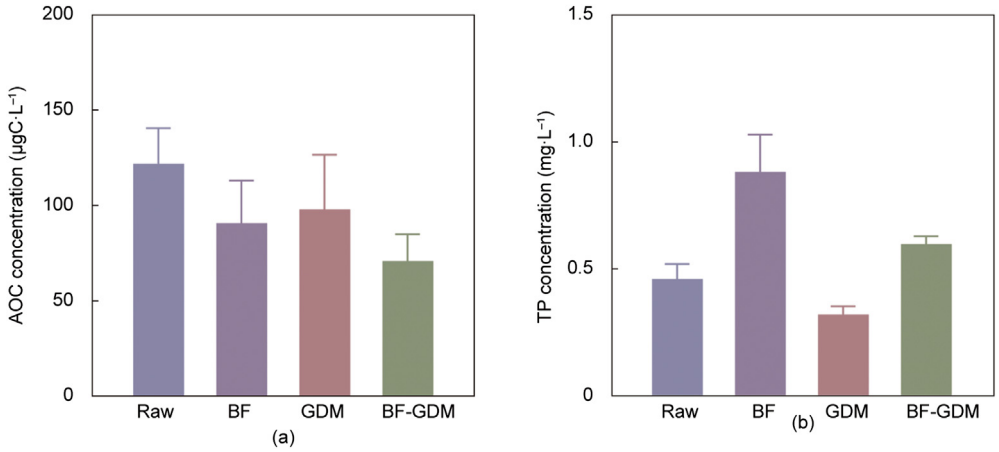

Fig. 5. Concentration of (a) AOC and (b) TP in the feedwater, the effluent of BF, and the permeate of GDM systems. The unit of ugC·L^{-1} is micrograms carbon per liter. n = 3, error bars represent the standard deviation.

3.2. Improving permeate biological stability by BF pretreatment

In the context of decentralized drinking water treatment, chlorine disinfection is sometimes a challenge [55]; thus, the distribution network may lack residual chlorine to prevent the regrowth of microorganisms. Consequently, enhancing the biological stability of the GDM permeates is crucial. AOC and P are closely related to bacterial regrowth [40,56]. AOC serves as a carbon substrate for microbial growth, and lower AOC levels may reduce the potential for bacterial regrowth. P is an essential component of bacterial cells and a crucial component for microbial growth [56]. Therefore, we investigated the removal effects of AOC and TP (Fig. 5). The removal efficiency of AOC was 19.7% in the control GDM. As BF pretreatment could remove 25.6% of the AOC, the total removal of AOC in BF-GDM was further increased to 41.8%. By decreasing P concentration in water, microbial regrowth can be controlled [57]. Control-GDM exhibited a TP removal efficiency of 30.3%. The result could be attributed to the potential involvement of phosphate-accumulating organisms (Proteobacteria and Bacteroidota) [58,59]. After BF pretreatment, the P concentration in the BF-GDM permeate increased, which may be due to the release of P from the filtration media during the BF process. The filtration media were sourced from a bank near the residential area of East Lake, which might have been heavily contaminated with P. To achieve a low P concentration in BF-GDM, a bank with lower P pollution could be chosen, and P adsorbents could be introduced into the BF [60]. In summary, BF enhanced the biological stability of the GDM permeate, thereby reducing the potential for microbial regrowth.

3.3. Enhancing stable flux in GDM system by BF pretreatment

During the initial phase of filtration (about 10 days), both control-GDM and BF-GDM exhibited notable decreases in the permeate flux and increased fouling resistance (Fig. 6 [6,8–12,61–64]). The control-GDM system experienced a larger flux drop than the BF-GDM system. After 30 d of operation, the control-GDM maintained a stable flux of 2.8 L·m^{-2}·h^{-1}. In contrast, the BF-GDM achieved a significantly higher stable flux of 7.3 L·m^{-2}·h^{-1}, indicating that the stable flux of the GDM system was markedly enhanced by the BF pretreatment. GDM generally achieved a flux of approximately 7 L·m^{-2}·h^{-1} only when the feedwater had a good quality (DOC < 3 mg·L^{-1}; Fig. 6(b) and Table S1 in Appendix A) [61]. In this study, raw water with a DOC concentration of 7.8 mg·L^{-1} resulted in a stabilized flux of 2.8 L·m^{-2}·h^{-1} for the GDM system. However, after BF pretreatment, although the DOC content was reduced by only approximately 20%, the stabilized flux increased by 2.6 times. This result might be ascribed to the fact that the BF pretreatment removed some crucial foulants such as POC (Fig. 2(b)), protein-like substances (Fig. 3(a)), and biopolymers (Fig. 3(b)).

The permeate flux greatly decreased on days 142–151 in both GDM systems (Fig. 6(a)). This decrease was caused by the addition of methanol solution in the raw water, causing the increase of feed DOC from 7.8 to 23.4 mg·L^{-1}. However, when the addition of methanol stopped, the permeate flux gradually returned to its initial level. Elevated DOC levels may facilitate the growth of microorganisms, ultimately resulting in severe biofouling. This is apparent from the development of a gel-like layer on the membrane surface. When the influent returns to its previous levels, the reduction in carbon sources inhibits microbial growth, thereby controlling biofouling. With limited carbon sources, the gel layer deposited on the membrane might act as an additional carbon source. Consequently, the gel layer gradually diminished, and the flux returned to its initial level. These findings suggest that the bio-cake layer possesses a certain degree of self-cleaning capability and that GDM can adapt to fluctuating water quality.

The fouling resistance composition was analyzed for both GDM systems after the experiment (Fig. 6(d)). Consistent with earlier studies, bio-cake layer resistance was found to be the primary factor contributing to fouling, accounting for 90.7% and 81.5% of the total fouling resistance in the control-GDM and BF-GDM systems, respectively [13,61]. This high proportion of bio-cake layer resistance relative to the total resistance allowed the achievement of a stable flux through a self-regulating bio-cake. Compared to the control-GDM with a bio-cake layer resistance of 7.8 × 10^{12} m^{-1}, the BF-GDM exhibited a significantly lower bio-cake layer resistance (2.2 × 10^{12} m^{-1}), and thus a much higher stable flux. Moreover, the pore-blocking resistance was reduced by approximately 40% with BF pretreatment, indicating that BF could effectively remove foulants that block membrane pores, such as hydrophobic organic matter [65]. In summary, the BF pretreatment substantially decreased both cake fouling and pore-blocking fouling.

3.4. Related the GDM performance to the characteristics of bio-cake layer

Fig. 6(d) indicates that the bio-cake layer was the primary contributor to membrane fouling resistance and influenced the effectiveness of the GDM system in pollutant removal. Thus, we attempted to provide an explanation for the improvement in GDM performance by examining the morphology, content, and microbial population of the bio-cake layer.

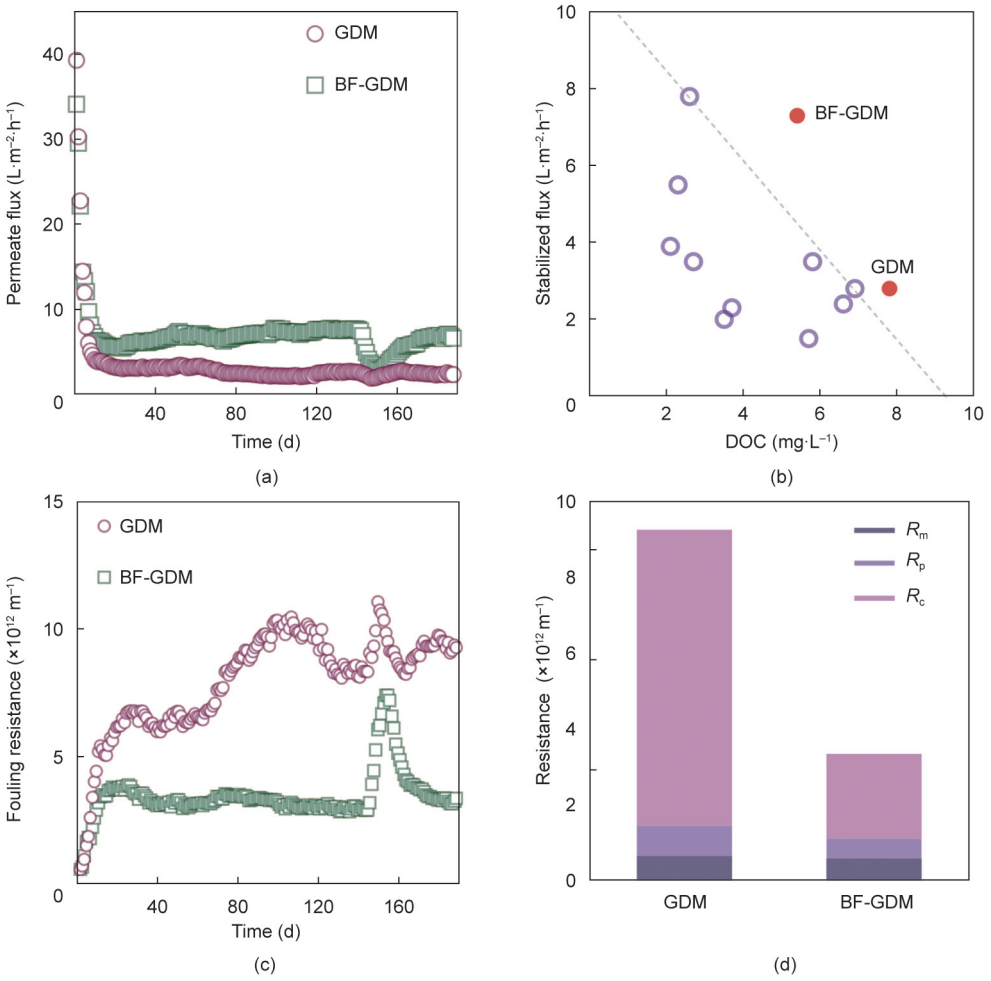

Fig. 6. Membrane performance in the control-GDM and BF-GDM. (a) Permeate flux; (b) comparison of the stabilized flux of the BF-GDM (indicated by solid circles) with that of the GDM in previous studies [6,8–12,61–64] (indicated by open circles); (c) fouling resistance; and (d) composition of fouling resistance. The sudden change of flux in days 142–151 was due to the addition of a methanol solution containing micropollutants into the raw water. Data in Fig. 6(b) are detailed in Table S1 in Appendix A.

3.4.1. Morphology of the bio-cake layers

To evaluate the effect of BF pretreatment on the bio-cake layers, we used *in situ* OCT imaging to examine their structure (Fig. 7). Both the control-GDM and BF-GDM systems exhibited bio-cake layers with rough and heterogeneous structures, which may have influenced flux stabilization [2]. After 100 days of operation, the bio-cake layer thickness was measured as 115 μm in the BF-GDM system and 159 μm in the control-GDM system (Fig. S3(a) in Appendix A). Besides, the top-view images also revealed that the BF-GDM had a thinner bio-cake layer compared to the control-GDM (Fig. S4 in Appendix A). This result can be explained by the BF pretreatment, which effectively reduced the levels of turbidity (Fig. 2(a)), POC (Fig. 2(b)), and biopolymers (Fig. 3(b)), resulting in reduced foulant deposition and thinner bio-cake layers. In addition to its small thickness, the BF-GDM bio-cake also had a higher relative roughness (Fig. S5 in Appendix A). Moreover, higher surface roughness led to lower hydraulic resistance of the bio-cake layer (Fig. 6(a) and Fig. S3(b)) [61]. During 142–151 days, a gel layer developed on the upper portion of the cake layer, which was largely attributed to elevated organic matter levels in raw water (Figs. 7(a-v) and (b-v)). From day 150 to 188, the bio-cake layer thickness decreased by 17.7% in the control-GDM system and by 27.3% in the BF-GDM system (Fig. S3(a)). When the feed water returned to its original state, the gel layer gradually disappeared (Figs. 7(a-vi) and (b-vi)).

3.4.2. Composition of the bio-cake layer

EPS significantly contributes to the enhanced fouling resistance of the bio-cake layer [61]. The EPS content in the bio-cake layer of the BF-GDM was 890.4 $mg·m^{-2}$, which is less than half of the 2799.2 $mg·m^{-2}$ found in the control-GDM (Fig. 8), suggesting a reduced fouling resistance in the BF-GDM system. EPS may originate from biopolymers in the influent or microbial secretions within the bio-cake [66]. BF effectively removed biopolymers from the influent (Fig. 3(b)), leading to a reduction in EPS levels in BF-GDM. Furthermore, BF reduces the AOC concentration in the influent, decreasing the microbial nutrient source, which may promote the consumption of EPS [67]. Microbial activity is crucial for the self-regulation of bio-cake [61]. The ATP concentrations in the bio-cake layer were 192.8 $nmol·m^{-3}$ in the BF-GDM and 175.5 $nmol·m^{-3}$ in the control-GDM. A higher concentration of microorganisms can effectively loosen the cake layer and consume organic compounds, thereby forming a cake layer with reduced resistance [5,61]. In addition to engineering the cake layer, these microorganisms can eliminate certain pollutants in the influent such as AOC (Fig. 5(a)) and micropollutants (Fig. 4) [50,61].

3.4.3. Shifts of eukaryotic and bacterial communities by BF pretreatment

Alpha diversity indices were employed to assess the richness and diversity of microbial communities in the BF filtration column

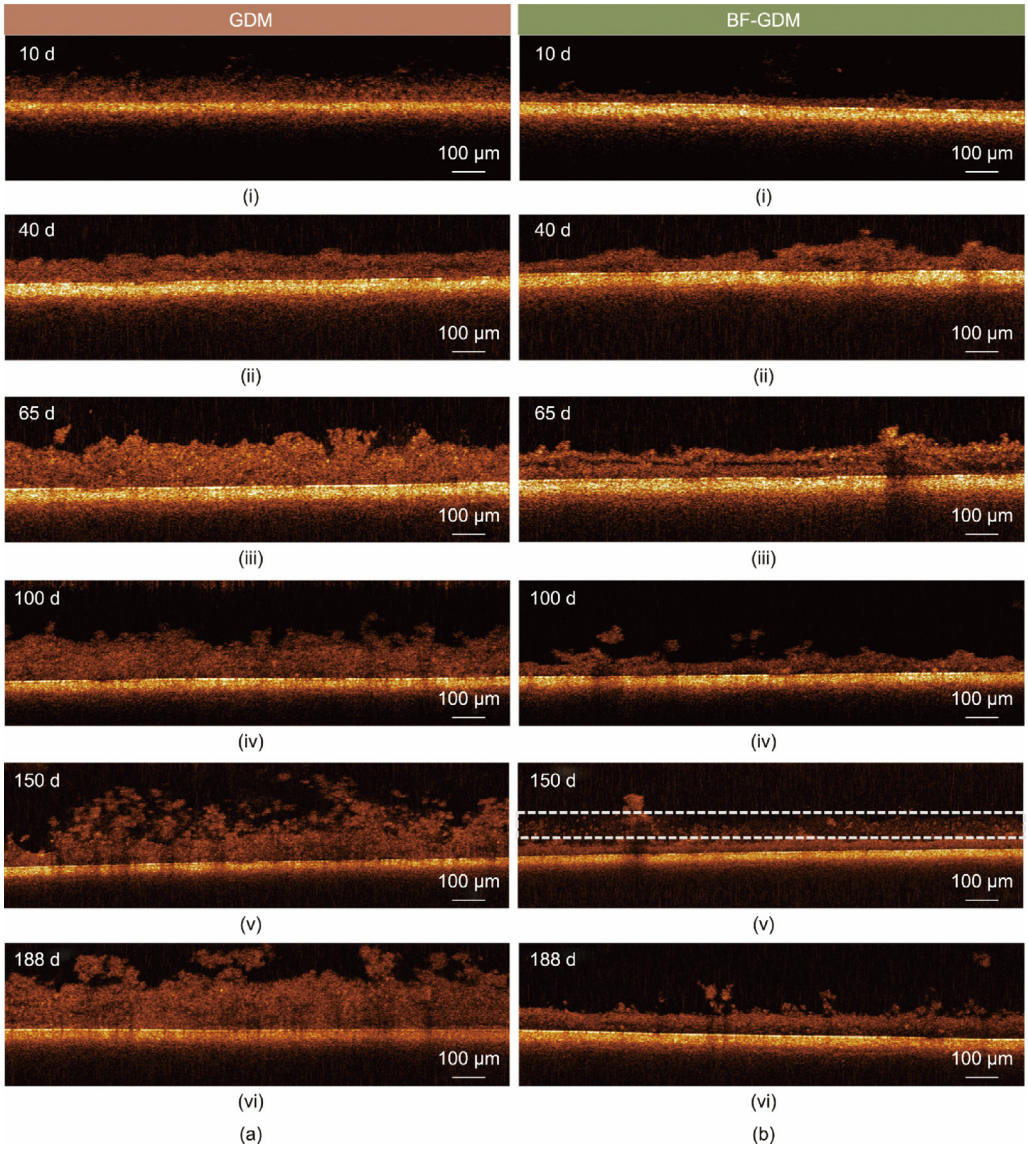

Fig. 7. Typical cross-sectional images depicting the bio-cake layers in the (a) control-GDM and (b) BF-GDM systems. These images are obtained *in situ* using OCT during the filtration.

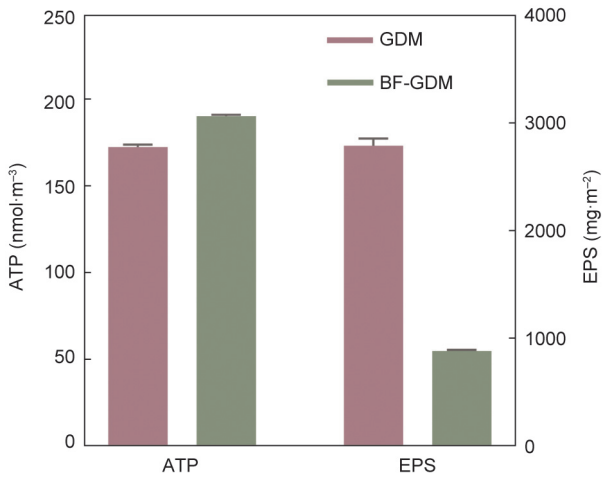

Fig. 8. Content of ATP and EPS in the bio-cake layers of the BF-GDM and control-GDM systems. n = 3, error bars represent the standard deviation.

and the bio-cake layer of the GDM systems (Fig. 9(a)). In BF-GDM, both Chao 1 and abundance-based coverage estimator (ACE) indices increased, suggesting that BF pretreatment enhanced bacterial community diversity of GDM. Furthermore, the increased Shannon index and decreased Simpson index suggested greater diversity within the bacterial community of BF-GDM than that of the control. The soil of banks contains a diverse range of microorganisms, some of which can pass through the BF into the GDM, thereby increasing the microbial abundance in the GDM. Microbial enrichment could help develop a more porous cake layer, which may improve the removal of targeted pollutants [68].

In most cases, the microbial microenvironment is shaped by the water quality [69]. We therefore analyzed the effect of pertinent physicochemical properties (DOC and AOC) of surface water on bacterial communities at the phylum level. CCA was employed using weighted UniFrac distances, as depicted in Fig. 9(b). CCA1 and CCA2 accounted for 72.3% and 27.7% of total variance, respectively. The length and direction of an environmental data arrow in the ordination plot reflect the correlation strength between the environmental data and community structure. In the GDM system,

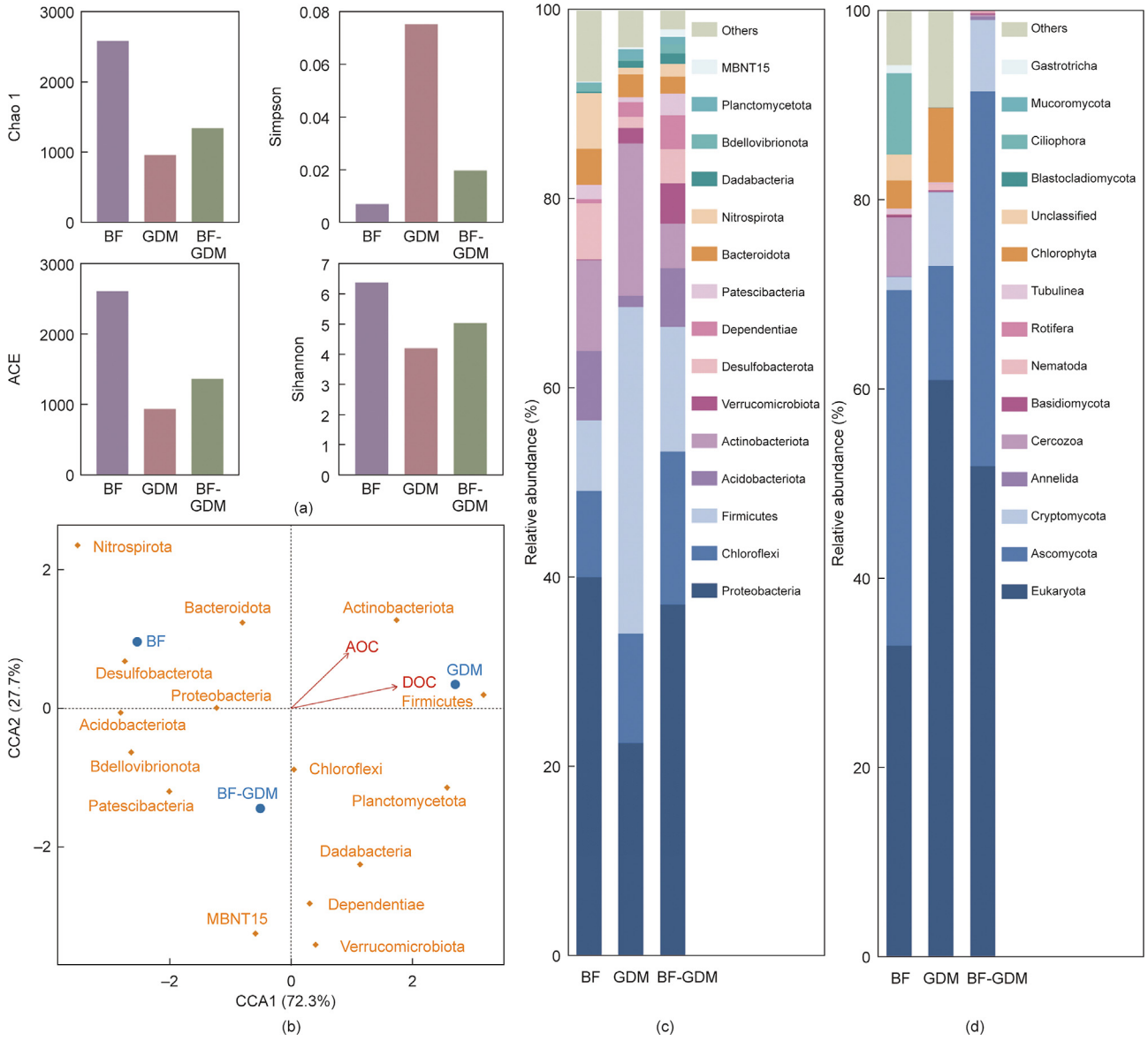

Fig. 9. Microbial community composition. (a) Alpha diversity in bacterial communities, including richness (Chao 1 and abundance-based coverage estimators (ACE)) and diversity (Shannon and Simpson). (b) CCA triplot examining ecological relationships between phylum-level microbial abundance and water quality parameters of AOC and DOC. (c) Composition of bacterial community at the phylum level and (d) eukaryotic community. Overall, 15 dominant microbial phyla are listed.

DOC was highly correlated with bacterial community composition, whereas in the BF-GDM system, DOC had minimal influence on the bacterial community composition. According to the length and direction of the environmental factors, there was a positive relationship between bacteria (Firmicutes and Actinobacteriota) and water quality (AOC and DOC), suggesting that the distribution of these species was influenced by AOC and DOC. Additionally, the bacterial communities associated with pollutant removal in the BF-GDM system exhibited a more concentrated distribution. In summary, BF increases both the abundance and diversity of bacterial communities, leading to a greater population of functional bacteria in the BF-GDM system, which is linked to better water quality.

Figs. 9(c) and (d) show the predominant bacterial and eukaryotic compositions at the phylum level. Although the dominant species across the BF, control-GDM, and BF-GDM systems had similar compositions, their relative abundances differed. Proteobacteria were the dominant phylum, comprising 40.0% of BF, 37.1% of BF-GDM, and 22.5% of control-GDM (Fig. 9(c)). Proteobacteria are commonly present in drinking water treatment systems because of their capacity for carbohydrate decomposition [70]. Bacteroidota and Nitrospirota were more abundant in the BF. These bacteria are involved in degrading biodegradable organic compounds in both dissolved and colloidal forms [14,58], which may lead to lower POC and AOC levels in the BF. In the eukaryotic community, Eukaryota were dominant in all three systems (Fig. 9(d)), and comparable findings have been reported [71,72]. These eukaryotes assist in creating a porous and heterogeneous bio-cake layer through predation and grazing. The relative abundances of *Bacillus* were lower in BF (2.5%) and BF-GDM (9.3%) compared to the control-GDM (25.5%) (Fig. S6 in Appendix A). *Bacillus* can produce EPS, which is detrimental to bio-cake layer resistance (Fig. 8) [73]. Overall, the BF removed various pollutants from the feedwater and added a wide range of microorganisms to the UF

membrane, resulting in a loose and porous bio-cake layer in the BF-GDM system.

4. Conclusions

In this study, we demonstrated that BF pretreatment significantly improves the performance of GDM systems, addressing key challenges of low flux and poor decontamination efficiency. Our findings lead to the following conclusions:

(1) BF could effectively enhance the permeate quality of GDM. BF effectively removed turbidity (55.3%) and POC (62.0%), which expanded the capability of GDM to purify high-turbidity raw water. Although BF only increased the removal of dissolved organic matter by approximately 20%, it greatly increased the removal of large molecular organic compounds and protein-like fluorescent substances. The removal efficiency of micropollutant also increased by 15.2%–65.3% in the BF-GDM system. Furthermore, BF enhanced the AOC removal in the BF-GDM system by 41.8%, thereby efficiently enhancing the biological stability of the permeate.

(2) BF could effectively alleviate membrane fouling and increase the stable flux of GDM. BF improved the stable flux of GDM from 2.8 to 7.3 $L \cdot m^{-2} \cdot h^{-1}$. This enhancement is likely due to the efficient removal of POC, biopolymers, and protein-like fluorescent substances from the raw water. The bio-cake layer of GDM with BF had a thinner and rougher morphology and a higher microbial density. Furthermore, the presence of BF enhanced microbial diversity and enriched functional microorganisms (such as Nitrospirota and Ascomycota) in the bio-cake layer.

Overall, BF pretreatment offers a low-maintenance, chemical-free, and sustainable strategy for improving both the efficiency and stability of GDM systems.

CRediT authorship contribution statement

Na Li: Writing – review & editing, Writing – original draft, Software, Methodology, Investigation, Formal analysis, Data curation. **Chu Zhou:** Validation, Investigation. **Fang Xu:** Visualization, Software. **Danting Shi:** Validation, Software. **Fanxi Zeng:** Validation, Project administration. **Liang Luo:** Software, Formal analysis. **Zheng Fang:** Methodology, Investigation. **Senlin Shao:** Writing – review & editing, Supervision, Project administration, Investigation, Funding acquisition, Conceptualization.

Declaration of competing interest

The authors declare that they have no known competing financial interests or personal relationships that could have appeared to influence the work reported in this paper.

Acknowledgments

This study was supported by the National Natural Science Foundation of China (52270077 and 52070147).

Appendix A. Supplementary data

Supplementary data to this article can be found online at https://doi.org/10.1016/j.eng.2025.01.003.

References

[1] Peter-Varbanets M, Margot J, Traber J, Pronk W. Mechanisms of membrane fouling during ultra-low pressure ultrafiltration. J Membr Sci 2011;377(1–2):42–53.
[2] Pronk W, Ding A, Morgenroth E, Derlon N, Desmond P, Burkhardt M, et al. Gravity-driven membrane filtration for water and wastewater treatment: a review. Water Res 2019;149:553–65.
[3] Zhou C, Luo YY, Xiong KY, Shao SL. A low-maintenance process for decentralized water purification using nanofiltration operated at ultralow flux. Separ Purif Tech 2023;327:124869.
[4] Boulestreau M, Hoa E, Peter-Verbanets M, Pronk W, Rajagopaul R, Lesjean B. Operation of gravity-driven ultrafiltration prototype for decentralised water supply. Desalin Water Treat 2012;42(1–3):125–30.
[5] Feng JY, Li X, Yang YL, Fan XY, Zhou ZW, Ren JW, et al. Insight into biofouling mechanism in biofiltration-facilitated gravity-driven membrane (GDM) system: beneficial effects of pre-deposited adsorbents. J Membr Sci 2022;662:121017.
[6] Li K, Xu WH, Han M, Cheng Y, Wen G, Huang TL. Integration of iron-manganese co-oxide (FMO) with gravity-driven membrane (GDM) for efficient treatment of surface water containing manganese and ammonium. Separ Purif Tech 2022;282:119977.
[7] Asif MB, Hai FI, Dhar BR, Ngo HH, Guo W, Jegatheesan V, et al. Impact of simultaneous retention of micropollutants and laccase on micropollutant degradation in enzymatic membrane bioreactor. Bioresour Technol 2018;267:473–80.
[8] Du P, Li X, Yang YL, Zhou ZW, Fan XY, Chang HQ, et al. Regulated-biofilms enhance the permeate flux and quality of gravity-driven membrane (GDM) by *in-situ*-coagulation combined with activated alumina filtration. Water Res 2022;209:117947.
[9] Shi DT, Liu Y, Fu WW, Li JY, Fang Z, Shao SL. A combination of membrane relaxation and shear stress significantly improve the flux of gravity-driven membrane system. Water Res 2020;175:115694.
[10] Du P, Li X, Yang YL, Zhou ZW, Fan XY, Feng JY. Algae-laden fouling control by gravity-driven membrane ultrafiltration with aluminum sulfate-chitosan: the property of floc and cake layer. Water 2020;12(7):1990.
[11] Huang YD, Cheng P, Tan FJ, Huang YJ, Li P, Xia SJ. Effect of coagulation pretreatment on the performance of gravity-driven membrane filtration with Yangtze River water. J Clean Prod 2021;297:126736.
[12] Shao SL, Shi DT, Li YQ, Liu Y, Lu ZY, Fang Z, et al. Effects of water temperature and light intensity on the performance of gravity-driven membrane system. Chemosphere 2019;216:324–30.
[13] Ding A, Wang JL, Lin DC, Zeng R, Yu SP, Gan ZD, et al. Effects of GAC layer on the performance of gravity-driven membrane filtration (GDM) system for rainwater recycling. Chemosphere 2018;191:253–61.
[14] Feng JY, Li X, Li H, Yang YL. Enhanced filtration performance of biocarriers facilitated gravity-driven membrane (GDM) by vacuum ultraviolet (VUV) pretreatment: membrane biofouling characteristics and bacterial investigation. J Membr Sci 2022;660:120859.
[15] Netcher AC, Duranceau SJ. Modeling the improvement of ultrafiltration membrane mass transfer when using biofiltration pretreatment in surface water applications. Water Res 2016;90:258–64.
[16] Lee S, Suwarno SR, Quek BWH, Kim L, Wu B, Chong TH. A comparison of gravity-driven membrane (GDM) reactor and biofiltration+ GDM reactor for seawater reverse osmosis desalination pretreatment. Water Res 2019;154:72–83.
[17] Yang CP, Qian H, Li X, Cheng Y, He HJ, Zeng GM, et al. Simultaneous removal of multicomponent VOCs in biofilters. Trends Biotechnol 2018;36(7):673–85.
[18] McCormick NE, Earle M, Ha C, Hakes L, Evans A, Anderson L, et al. Biological and physico–chemical mechanisms accelerating the acclimation of Mn-removing biofilters. Water Res 2021;207:117793.
[19] Hatt BE, Fletcher TD, Deletic A. Hydraulic and pollutant removal performance of fine media stormwater filtration systems. Environ Sci Technol 2008;42(7):2535–41.
[20] Siriwardene NR, Deletic A, Fletcher T. Clogging of stormwater gravel infiltration systems and filters: insights from a laboratory study. Water Res 2007;41(7):1433–40.
[21] D'Alessio M, Yoneyama B, Ray C. Fate of selected pharmaceutically active compounds during simulated riverbank filtration. Sci Total Environ 2015;505:615–22.
[22] Grützmacher G, Wessel G, Klitzke S, Chorus I. Microcystin elimination during sediment contact. Environ Sci Technol 2010;44(2):657–62.
[23] Hallé C, Huck PM, Peldszus S, Haberkamp J, Jekel M. Assessing the performance of biological filtration as pretreatment to low pressure membranes for drinking water. Environ Sci Technol 2009;43(10):3878–84.
[24] Bayarsaikhan U, Ruhl AS, Jekel M. Characterization and quantification of dissolved organic carbon releases from suspended and sedimented leaf fragments and of residual particulate organic matter. Sci Total Environ 2016;571:269–74.
[25] Zeeshan M, Ali O, Tabraiz S, Ruhl AS. Seasonal variations in dissolved organic matter concentration and composition in an outdoor system for bank filtration simulation. J Environ Sci 2024;135:252–61.
[26] Zeeshan M, Klitzke S, Ruhl AS. Changes in dissolved organic matter and oxygen consumption in different bank filtration simulations at different scales. Environ Sci Water Res Technol 2023;9(7):1862–2189.
[27] Cheng X, Hou C, Gao H, Li P, Zhu X, Luo C, et al. Synergistic process using calcium peroxide and ferrous iron for enhanced ultrafiltration of microcystis aeruginosa-laden water. Water Res 2022;211:118067.
[28] Chen F, Peldszus S, Elhadidy AM, Legge RL, Van Dyke MI, Huck PM. Kinetics of natural organic matter (NOM) removal during drinking water biofiltration

using different NOM characterization approaches. Water Res 2016;104:361–70.
[29] Huber SA, Balz A, Abert M, Pronk W. Characterisation of aquatic humic and non-humic matter with size-exclusion chromatography–organic carbon detection–organic nitrogen detection (LC–OCD–OND). Water Res 2011;45(2):879–85.
[30] Bray RT, Jankowska K, Kulbat E, Luczkiewicz A, Sokolowska A. Ultrafiltration process in disinfection and advanced treatment of tertiary treated wastewater. Membranes 2021;11(3):221.
[31] Zhao J, Fang S, Qi W, Liu H, Qu J. Do NH_4^+-N and AOB affect atenolol removal during simulated riverbank filtration? Chemosphere 2022;301:134653.
[32] Bai Y, Ruan XH, Wang FF, Antoine G, van der Hoek JP. Sulfonamides removal under different redox conditions and microbial response to sulfonamides stress during riverbank filtration: a laboratory column study. Chemosphere 2019;220:668–77.
[33] Shao SL, Liang H, Qu FS, Yu HR, Li K, Li GB. Fluorescent natural organic matter fractions responsible for ultrafiltration membrane fouling: identification by adsorption pretreatment coupled with parallel factor analysis of excitation–emission matrices. J Membr Sci 2014;464:33–42.
[34] Lian JC, Zhang LJ, Tan FX, Xu JT, Mu RM, Wu DJ, et al. Enhancing ultrafiltration of algal-rich water using ferrate activated with sodium percarbonate: foulants variation, membrane fouling alleviation, and collaborative mechanism. Chemosphere 2022;308:136377.
[35] Trulleyová S, Rulík M. Determination of biodegradable dissolved organic carbon in waters: comparison of batch methods. Sci Total Environ 2004;332(1–2):253–60.
[36] Hammes FA, Egli T. New method for assimilable organic carbon determination using flow-cytometric enumeration and a natural microbial consortium as inoculum. Environ Sci Technol 2005;39(9):3289–94.
[37] Derlon N, Mimoso J, Klein T, Koetzsch S, Morgenroth E. Presence of biofilms on ultrafiltration membrane surfaces increases the quality of permeate produced during ultra-low pressure gravity-driven membrane filtration. Water Res 2014;60:164–73.
[38] Shao SL, Li YQ, Jin TC, Liu WS, Shi DT, Wang J, et al. Biofouling layer maintains low hydraulic resistances and high ammonia removal in the UF process operated at low flux. J Membr Sci 2020;596:117612.
[39] Cruz de Carvalho MH, Sun HX, Bowler C, Chua NH. Noncoding and coding transcriptome responses of a marine diatom to phosphate fluctuations. New Phytol 2016;210(2):497–510.
[40] Vrouwenvelder JS, Beyer F, Dahmani K, Hasan N, Galjaard G, Kruithof JC, et al. Phosphate limitation to control biofouling. Water Res 2010;44(11):3454–66.
[41] Gilcreas FW. Standard methods for the examination of water and waste-water. Am J Public Health Nations Health 1966;56(3):387–8.
[42] Hammes F, Goldschmidt F, Vital M, Wang YY, Egli T. Measurement and interpretation of microbial adenosine tri-phosphate (ATP) in aquatic environments. Water Res 2010;44(13):3915–23.
[43] Ahokas H, Naskali L. Bicinchonic acid protein assay reveals high-lysine contents in barley seed protein extracts. J Cereal Sci 1988;7(1):43–8.
[44] Chang CL, Liao CS. Assessing the risk posed by high-turbidity water to water supplies. Environ Monit Assess 2012;184(5):3127–32.
[45] Lee S, Suwarno SR, Quek BWH, Kim L, Wu B, Chong TH. A comparison of gravity-driven membrane (GDM) reactor and biofiltration plus GDM reactor for seawater reverse osmosis desalination pretreatment. Water Res 2019;154:72–83.
[46] Tang XB, Pronk W, Ding A, Cheng XX, Wang JL, Xie BH, et al. Coupling GAC to ultra-low-pressure filtration to modify the biofouling layer and bio-community: flux enhancement and water quality improvement. Chem Eng J 2018;333:289–99.
[47] Li D, He H, Jia J, Shi W, Yin F, Yu J, et al. Mitigation of ultrafiltration membrane fouling by a simulated sunlight-peroxymonosulfate system with the assistance of irradiated NOM. Water Res 2023;229:119452.
[48] Tian JY, Liang H, Li X, You SJ, Tian S, Li GB. Membrane coagulation bioreactor (MCBR) for drinking water treatment. Water Res 2008;42(14):3910–20.
[49] Zhao YX, Liu D, Huang WL, Yang Y, Ji M, Nghiem LD, et al. Insights into biofilm carriers for biological wastewater treatment processes: current state-of-the-art, challenges, and opportunities. Bioresour Technol 2019;288:121619.
[50] Tang X, Zhu X, Huang K, Wang J, Guo Y, Xie B, et al. Can ultrafiltration singly treat the iron- and manganese-containing groundwater? J Hazard Mater 2021;409:124983.
[51] Ruppelt JP, Pinnekamp J, Tondera K. Elimination of micropollutants in four test-scale constructed wetlands treating combined sewer overflow: influence of filtration layer height and feeding regime. Water Res 2020;169:115214.
[52] Nure JF, Nkambule TTI. The recent advances in adsorption and membrane separation and their hybrid technologies for micropollutants removal from wastewater. J Ind Eng Chem 2023;126:92–114.
[53] Huang SQ, Voutchkov N, Jiang S. Balancing carbon, nitrogen and phosphorus concentration in seawater as a strategy to prevent accelerated membrane biofouling. Water Res 2019;165:114978.
[54] Pandey B, Pandey AK, Tripathi K, Dubey SK. Biodegradation of acetaminophen: microcosm centric genomic-proteomic-metabolomics evidences. Bioresour Technol 2024;401:130732.
[55] Bai XH, Zhi XH, Zhu HF, Meng MQ, Zhang MD. Real-time ArcGIS and heterotrophic plate count based chloramine disinfectant control in water distribution system. Water Res 2015;68:812–20.
[56] Yang Y, Lohwacharin J, Takizawa S, Hou LA. Comparison between ferrihydrite adsorption and full-scale advanced drinking water treatment processes for controlling bacterial regrowth potential. Chemosphere 2020;241:125001.
[57] Xing XC, Li T, Bi ZH, Qi P, Li ZS, Chen YY, et al. Destruction of microbial stability in drinking water distribution systems by trace phosphorus polluted water source. Chemosphere 2021;275:130032.
[58] He Q, Yan X, Fu Z, Zhang Y, Bi P, Mo X, et al. Rapid start-up and stable operation of an aerobic/oxic/anoxic simultaneous nitrification, denitrification, and phosphorus removal reactor with no sludge discharge. Bioresour Technol 2022;362:127777.
[59] Zhao X, Xie YL, Sun B, Liu Y, Zhu SM, Li W, et al. Unraveling microbial characteristics of simultaneous nitrification, denitrification and phosphorus removal in a membrane-aerated biofilm reactor. Environ Res 2023;239:117402.
[60] Lee JI, Kim JM, Yoo SC, Jho EH, Lee CG, Park SJ. Restoring phosphorus from water to soil: using calcined eggshells for P adsorption and subsequent application of the adsorbent as a P fertilizer. Chemosphere 2022;287:132267.
[61] Shi DT, Zeng FX, Gong TJ, Li JY, Shao S. Iron amended gravity-driven membrane (IGDM) system for heavy-metal-containing groundwater treatment. J Membrane Sci 2022;643:120067.
[62] Li WH, Siddique MS, Graham N, Yu WZ. Influence of temperature on biofilm formation mechanisms using a gravity-driven membrane (GDM) system: insights from microbial community structures and metabolomics. Environ Sci Technol 2022;56:8908–19.
[63] Tang XB, Pronk W, Traber J, Liang H, Li GB, Morgenroth E. Integrating granular activated carbon (GAC) to gravity-driven membrane (GDM) to improve its flux stabilization: respective roles of adsorption and biodegradation by GAC. Sci Total Environ 2021;768:144758.
[64] Tang XB, Xie BH, Chen R, Wang JL, Huang KJ, Zhu XW, et al. Gravity-driven membrane filtration treating manganese-contaminated surface water: flux stabilization and removal performance. Chem Eng J 2020;397:125248.
[65] Lin L, Zhang Y, Fu BG, Yan WX, Fu Q, Li S. Pre-depositing versus mixing powdered activated carbons for gravity-driven membrane systems during treated domestic wastewater filtration: permeability stabilization and removal performance. Separ Purif Tech 2022;288:120659.
[66] Li J, Hao XD, Gan W, van Loosdrecht MCM, Wu YY. Recovery of extracellular biopolymers from conventional activated sludge: potential, characteristics and limitation. Water Res 2021;205:177706.
[67] Tang XB, Ding A, Pronk W, Ziemba C, Cheng XX, Wang JL, et al. Biological pre-treatments enhance gravity-driven membrane filtration for the decentralized water supply: linking extracellular polymeric substances formation to flux stabilization. J Clean Prod 2018;197:721–31.
[68] Chen R, Liang H, Wang JL, Lin DC, Zhang H, Cheng XX, et al. Effects of predator movement patterns on the biofouling layer during gravity-driven membrane filtration in treating surface water. Sci Total Environ 2021;771:145372.
[69] Su ZY, Liu T, Men Y, Li S, Graham N, Yu WZ. Understanding point-of-use tap water quality: from instrument measurement to intelligent analysis using sample filtration. Water Res 2022;225:119205.
[70] Frank VB, Regnery J, Chan KE, Ramey DF, Spear JR, Cath TY. Co-treatment of residential and oil and gas production wastewater with a hybrid sequencing batch reactor–membrane bioreactor process. J Water Process Eng 2017;17:82–94.
[71] Lee S, Sutter M, Burkhardt M, Wu B, Chong TH. Biocarriers facilitated gravity-driven membrane (GDM) reactor for wastewater reclamation: effect of intermittent aeration cycle. Sci Total Environ 2019;694:133719.
[72] Akhondi E, Wu B, Sun SY, Marxer B, Lim WK, Gu J, et al. Gravity-driven membrane filtration as pretreatment for seawater reverse osmosis: linking biofouling layer morphology with flux stabilization. Water Res 2015;70:158–73.
[73] Sun LQ, Lin WC, Li DY, Xiao K, Chen DY, Luo S, et al. Significant insights of Cu and Fe as key metals to cause RO membrane fouling under coal-mining wastewater treatment. Desalination 2023;555:116517.